Relationship of VOCs and NO_X to photochemical ozone production by one year observational data in Guangzhou, China

Y. Zou[1,2], X. J. Deng[1,2], B. G. Wang[2], F. Li[1], H. B. Tan[1], T. Deng[1], B. R. Mai[1], and X. T. Liu[1]

[1]Institute of Tropical and Marine Meteorology/Guangdong Provincial Key Laboratory of Regional Numerical Weather Prediction, CMA, Guangzhou, China

[2]Institute of Atmospheric Environmental Safety and Pollution Control, Jinan University, Guangzhou, China

Received: 3 June 2014 – Accepted: 21 June 2014 – Published:

Correspondence to: X. J. Deng (dxj@grmc.gov.cn) and B. G. Wang (bongue@126.com)

Published by Copernicus Publications on behalf of the European Geosciences Union.

Abstract

In this study, online monitoring instruments were used to monitor the ozone, NO_x and VOCs from the Guangzhou Panyu Atmospheric Composition Station (GPACS) of the China Meteorological Administration from June 2011 to May 2012, so as to obtain their characterizations and relationships of VOCs and NOx to photochemical ozone production. The results show that during the observation period, the seasonal variation of ozone concentration was lower in spring and winter, while being higher in summer and autumn, which is contrary that of the VOCs and NOx. Aromatics are the largest components for ozone formation potential, among which toluene, m-xylene, p-xylene and 1,3,5-trimethylbenzene are the most important components, with a total contribution of approximately 31.6% to ozone formation potential. The peak ozone during high-concentration ozone events is found to be NOx-limited by measured O_3 isopleths diagram and further confirmed by measured VOC/NOx, which provides the ozone control strategy which involves, in addition to the control of VOCs emissions, increased emphasis on reducing NOx emissions, to achieve the purpose of controlling high-concentration ozone

1 Introduction

Along with its rapid economic development and urbanization, the Pearl River Delta has become one of the most serious pollution areas in China (Chan et al., 2008). Different from the air pollution situations of Beijing, Tianjin, Hebei and the Yangtze River Delta region, which involve particulate matters as the main pollutants (Wang et al., 2012; Zhao et al., 2011), due to its unique geographical location and climate, as well as the rapid increase in the emissions of VOCs and NO_x ($NO+NO_2$) as ozone precursors caused by industrial activities and the growing number of motor vehicles, in the Pearl River Delta high-concentration ozone events occur frequently and have become very prominent air pollution problems (Wang et al., 2009). Tropospheric ozone is the secondary pollutant generated by photochemical reactions of VOCs and NO_x under light conditions (Sillman, 1995). However, VOCs and NO_x have no linear relationship with ozone formation, and their impacts on ozone formation can be described by VOC and NO_x limited regime (Zhang et al., 2004; Tie et al., 2007; Geng et al., 2008). A large amount of research has been conducted regarding ozone formation in the Pearl River Delta (Wang et al.,2005; Cheng et al.,2010;Guo et al.,2009). Many laboratory studies using smog chambers have served to clarify the gas-phase photochemical transformations of NOx and VOCs, and their roles in the formation of ozone. The maximum ozone concentrations generated from various mixtures of NOx and VOCs are often presented on ozone isopleths diagrams. The numerical simulations showed that although the specific actual situations differ, it is generally considered that when the VOC/NOx ratio is greater than 8:1, ozone formation regime is NOx-limited, while the VOC/NOx ratio is less than 8:1, ozone formation regime is VOC-limited (Dodge,1977), which many researchers have used to elucidate the characteristics of photochemical ozone production(Sillman,1999;Committee on Tropospheric Ozone Formation and Measurement,1991; Ran et al.,2009 , 2011). However, little attention has been given to ozone isopleths diagrams and VOC/NOx ratio using observational data. In addition, most previous studies performed in the Pearl River Delta region reported that the ozone is VOC-limited(Zhang et al., 2008b; Guo et al., 2009).However, few previous studies on the region's ozone formation regime have examined the possible diurnal variations in ozone formation regime.

Currently, a greater amount of systematic long-term observation data on atmospheric ozone and NOx in the Pearl River Delta region has become available, while VOCs data which mostly involves short-term intensive observations or non-continuous long term observations is not included in the scope of daily observations (Wang et al., 2004; Shao et al., 2009). Therefore, the relationship among VOCs, NO_x and ozone cannot be fully revealed to discern the impacts of VOCs and NO_x on ozone formation in the Pearl River Delta region. In order to more effectively solve the problem of ozone pollution in the Pearl River Delta, VOCs, NO_x and ozone were observed throughout the period of one year at GPACS, focusing on analyzing the characterizations of VOCs, NOx and ozone. as well as VOCs components in ozone formation. In addition, ozone isopleths diagram using observational data is plotted to elucidate the characteristics of photochemical ozone productions, which can provide the policy of controlling the ozone in Guangzhou. Finally, the VOC/NOx ratio by observational data was also used to analyze the ozone formation regime with diurnal variation in Guangzhou, but this has only been done by a small number of scholars (Li et al., 2008). In order to reveal the occurrence of high-concentration ozone events in Guangzhou, ozone

formation regime with diurnal variation are explored in four scenarios herein, i.e. spring, summer, autumn and winter.

This study is organized as follows. The second section describes the methodology used in this study, also including the sampling point and observation instruments. The third section mainly analyzes the observed results, including characteristic analysis of ozone, NO_x and VOCs, as well as an analysis of the contribution of VOCs components to ozone formation by using MIR and an equivalent propylene concentration method. In the final section, the ozone isopleths diagram by observational data is plotted to elucidate the characteristic of photochemical ozone production, and the VOC/NO_x ratio analysis method is also adopted to analyze ozone formation regime in the seasonal diurnal variation process, in order to explore the ozone control strategies in Guangzhou.

2 Methodology

2.1 Measurements

From June 2011 to May 2012, automatic sampling and on-line monitoring were carried out on ozone, NO_x and VOCs. The sampling site was located at the mountain top of Dazhengang, Nancun Town, Panyu District, Guangzhou City, Guangdong Province, China with an elevation of 141 m, at the latitude of 23° 00.236′ N and longitude of 113° 21.292′ E (Fig. 1). This sampling station is located in suburban Guangzhou in which the high ozone events often occur, and is the main site of the observation network for atmospheric composition in Pearl River Delta. Fig.2 shows that, regardless of the large variation in concentration of the three types of VOCs, the relative contribution of the three groups remains fairly uniform throughout the observational time. Such uniformity implies that air was sufficiently homogenized from various point sources at the surface. The prevailing wind, wind speed and temperature at the sampling point during the different seasons are shown in Fig. 3 and Table 1. At the sampling point, northeasterly and southwesterly are the prevailing winds in spring (April, May and June), along with southwesterly in summer (June, July and August), southwesterly in autumn (September, October and November), and northeasterly in winter (December, January and February). In the different seasons, the average wind speed varies at around 1.4 ms^{-1}, while the average temperature undergoes more significant changes from 14.2 ℃ in winter to 29.4 ℃ in summer. Typical air pollution processes can also be seen in different seasons and under different weather conditions. When the prevailing wind is northeasterly in December, the difference between weekends and weekdays for VOCs is very typical, showing large amounts of pollutants are emitted from downtown Guangzhou City. When the prevailing wind is southwesterly in July, the difference between weekends and weekdays for VOCs is not apparent, for the reason that only small amounts of pollutants are emitted from the further suburban areas (Fig. 1).

2.2 Instrument description

The data used in this study include the hourly concentration of ozone, NO_x and VOCs during the observation period (June 2011–May 2012). The concentration of ozone gas was obtained using an EC9810B ozone analyzer produced by Ecotech Co. of Australia with the UV photometric method. The concentration of nitrogen oxides gas was collected using an EC9841B oxynitride ($NO/NO_2/NO_x$) gas analyzer produced by Ecotech with the chemiluminescence method.VOCs concentration was obtained using a GC5000 analyzer produced by AMA Co. of Germany with the GC-FID analysis method. This latter apparatus is

comprised of a low-boiling- point VOC analyzer and high-boiling-point BTX analyzer, including two sets of sampling systems and two systems of separated chromatographic columns. A low-boiling- point VOC analyzer was able to conduct enriched concentration on a tube which is filled with special adsorption materials at 13 ℃, a second adsorption at 20 ℃ and desorption when the temperature was raised to 200 ℃, followed by separation with two-dimensional chromatographic columns. The chromatographic columns consisted of a Al_2O_3/Na_2SO_4 plot column with a diameter of 0.32 mm, film thickness of 5mm and length of 60 m, as well as a back flushing column (carbowax) with a diameter of 0.32 mm, film thickness of 0.25mm and length of 30 m. A back flushing column was used to remove the moisture component and high boiling component, and two types of chromatographic column were polar columns. Through two rounds of thermal desorption, the low-boiling-point hydrocarbons could be well separated, and the detector was a flame ionization detector (FID). A BTX high-boiling-point analyzer was able to conduct precondensation of volatile organic compounds at 30℃, followed by thermal desorption, then separation on the DB-1 column to achieve optimum separation and prevent interference of related compounds. This column has a diameter of 0.32 mm, thickness of 10mm and length of 60 m. A flame ionization detector (FID) was used to detect the system. The detected target compounds were 56 types of VOCs designated by the US EPA with the time resolution of once per hour, and the standards we used were the same as those used by the EPA/USA PAMs(Photochemical Assessment Monitoring Stations)The analytical method was described in a previous study (Zou et al., 2013). The QA/QC of online VOC measurements was performed. Before and after the observation period, we performed a zero gas check for memory effect or contamination and a span gas check with PAMs calibration gas in order to check the drift, repeatability and memory effects. We normally got standard curve which qualified the species by using a five point calibration method and retention time which quantified the species. The standard curve and the detection line of VOCs are listed in Table 2. You can see that correlation coefficient ranged from 0.984 to 0.999, and detection limit ranged from 0.03ppbv to 0.09ppbv. During the observation period, we also performed a span gas check every month by using one point calibration and adjust the retention time. Finally, outliers need to be eliminated to guarantee the valid data.

3 Results and discussion

3.1 Characteristics of ozone, NO_x and VOCs

The seasonal diurnal variation characteristics of ozone, VOCs and NO_x are shown in Fig. 4 The seasonal variation characteristics of ozone are relatively apparent. The seasonal variation of ozone concentrations displays the seasonal pattern of being lower in the spring and winter and higher in the summer and autumn. Furthermore, the increase range is much larger in late spring and early summer than the other periods, which is mainly due to the light, temperature, other meteorological factors and emissions strength of air pollutants being different in each season (Bloomer et al., 2009, 2010). The seasonal variation in the concentration of ozone precursors is opposite to that of ozone concentration. NO_x concentration is higher in spring and winter, but lower in summer and autumn and VOCs concentration is higher in winter, but lower in summer. Average concentration of VOCs, NOx and ozone in four seasons are shown in Table 3.VOCs concentration varies from 34.60 ppbv in March to 63.57 ppbv in November; NOx concentration varies from 21.75 ppbv in August to 76.39 ppbv in March; and ozone

concentration varies from 9.31 ppbv in January to 29.67 ppbv in September.The diurnal concentration variation of ozone is unimodal, reaching its maximum at 2.00 p.m., while those of the ozone precursors, i.e. VOCs and NO_x, show a bimodal variation with a peak during rush hours, though variations may be not apparent among some seasons. These diurnal concentration variations exhibit the photochemical characteristic that photochemical precursors gradually reduce and products increase accordingly. In order to further understand the variation in ozone concentration and reveal its dependence on photochemical reactions, it is necessary to analyze the variation trend of ozone, shown as follows:

$$d[O_3]/dt = [O_3](t+1h) - [O_3](t) \quad (1)$$

In the equation, $[O_3](t)$ represents the ozone concentration at time t, and $[O_3](t+1h)$ is the ozone concentration for the next hour of time t. A negative growth of variation in ozone concentration indicates that the chemical loss of ozone plays a dominant role in the variation in ozone concentration, while the contrary indicates the fact that the generation of ozone photochemical reactions plays a key role. The results show that a negative growth of ozone concentration occurs between 15:00-18:00LT and 19:00-23:00LT. The first period of time(15:00-18:00LT) is presumably due to low OH radicals and the fact that titration of ozone by emissions of NOx plays a key role. However, during the second period of time(19:00-23:00LT), there was no OH radicals and the NO titration could still consume the ozone, until the NO titration ceased, the ozone concentration remained a relatively stable during the period (0:00-7:00LT).The concentration trend of ozone shows a positive growth during the period of time（8:00-14:00LT）due to the high OH radicals and strong photochemical reaction. (Fig. 5).

3.2 The effect of each VOCs category on ozone formation

VOCs appear in various types, and their concentrations do not correspond to their ozone formation. Different types of VOCs have different photochemical reactivities, thereby leading to different ozone formation potential. Controlling the species with the largest ozone formation potential is the most cost-effective solution to ozone control. VOCs have two main factors for ozone formation potential: kinetic activity and mechanism activity. on ozone formation. For kinetic activity, the propylene-equivalent concentration method (C_{PE} (J)) is expressed as shown below:

$$C_{PE}(J) = C_J K_{OH}(J)/K_{OH}(C_3H_6) \quad (2)$$

In the equation, J represents a species of VOC, C_J represents the carbon-number concentration (ppbc) of this species, and $K_{OH}(J)$ and $K_{OH}(C_3H_6)$ denote the chemical reaction rate constant in the free radical reaction of species J and propylene with OH. The reaction rate constants are shown in Table 4. For the mechanism activity, the MIR factor weighting method is used with the following expression:

$$Con_{j.MIR} = MIR \times Com_{ppbv} \times u_j/u_{ozone} \quad (3)$$

In the equation, u_j and u_{ozone} represent the relative molecular mass of species J in the VOCs and ozone respectively, Com_{ppbv} represents the actual volume mixing ratio, the Maximum Incremental Reactivity (MIR) factors were developed by Carter (Carter et al., 1994) in model Scenarios, the MIR of each VOCs is from numerical simulations, and $Con_{j.MIR}$ is maximum-increment-activity MIR factor weighting concentration which represents the maximum ozone concentration generated by this species based on MIR. The maximum ozone concentrations of the different VOCs are used to compare their relative ozone formation

potential. The MIR coefficients are shown in Table 4. Fig. 6 shows the characteristic of each VOCs category obtained at the sampling point by using the volume mixing ratio concentration (ppbv), carbon number concentration (ppbc), propylene-equivalent concentration (ppbc), and maximum-increment activity MIR factor weighting concentration (ppbv) methods. As viewed from the volume mixing ratio concentration (ppbv) and carbon concentration (ppbc) , alkanes occupy the largest proportion, accounting for 59% and 53% of the total VOCs concentration respectively; followed by aromatics(24% and 36% respectively); and alkenes have the lowest proportion, at 17% and 11% respectively. As viewed from the propylene-equivalent and MIR factor weighting concentrations, the alkenes and aromatics are dominant, accounting for total proportions of 73% and 83% respectively, and alkanes have the lowest proportion. Total propylene-equivalent concentration accounts for nearly half of the total carbon concentration, indicating that the activities of major VOCs species are lower than propylene at the sampling point. In summary, during the monitoring period, as viewed from the volume mixing ratio and carbon number concentrations of VOCs, alkanes and aromatics are shown to be the most important categories of the atmosphere at the sampling point. However, as viewed from ozone formation potential, aromatics and alkenes are the two species with the largest contributions. The alkanes content are high, but because of their low reactivity, alkanes have less contribution to the reactivity of VOCs and ozone formation potential. Although the alkenes concentrations are smaller than those of the alkanes, due to their high reactivity, alkenes have greater contributions to ozone than alkanes. Table 5 shows the ozone formation potential ranking of VOCs species as calculated by the propylene-equivalent concentration and MIR factor methods. It can be seen that the results of both methods are partially consistent, but some differences may also be seen. Among the top ten species, eight species are exactly the same, differing only in terms of rank order. It is thus shown that both methods can be used to reflect the ozone formation potential of each VOCs species to some extent, and especially those with greater contributions to ozone formation have better consistency. However, since these two methods differ in principle, the calculated ranks of ozone formation potential are also different. The propylene-equivalent concentration method only considering kinetic activity ignores the differences in the mechanism activities of the reaction between peroxide radicals and NO, thus when assessing ozone formation potential, the species with faster OH reaction rate may be overestimated, such as isoprene. Although the MIR factor method considers the kinetics and mechanism activity, due to the fact that the MIR factor involves possible uncertainty and lack of MIR data for some species, the MIR factor method cannot become a reliable assessment approach of ozone formation potential. In summary, aromatics are the species with the highest reactivity at the sample point, followed by alkenes. Toluene, m-xylene, p-xylene and 1,3,5-trimethylbenzene with higher reactivity have a total contribution to ozone formation potential of about 31.61 %. These species are mainly sourced from large factories and industrial activities (Liu et al., 2008a). As an industrial city, Dong guan is presumed to have some contributions to these species at sampling points in the autumn and winter, due to the fact that it is located in the eastern part of the sampling site and northeasterly is the prevailing in the autumn and winter at the sampling site. Moreover, isoprene has no high concentration, but ranks at first and third in terms of OH activity and MIR. Therefore, the choice of green plant species must consider the isoprene emissions of plants in the greening process at the

sampling point.

3.3 Ozone formation regime

VOCs and NO_x have a non-linear relationship with the formation of the ozone as a secondary photochemical product, and their impacts on the ozone formation can be described by the VOCs and NOx control areas. The peak ozone concentrations generated from various initial concentrations of NOx and VOCs are usually presented as an O_3 isopleth diagram, in which initial mixture compositions giving rise to the same peak O_3 concentrations are connected by the appropriate isopleth. O_3 isopleth diagrams can be generated for different VOCs and NOx mixtures and for different levels of solar intensity from modeling studies using the validated chemical mechanisms (Dodge, 1977).To elucidate the photochemical potential to produce ozone in Guangzhou City, observational data selected by meteorological conditions are used to plot the O_3 isopleths diagrams. Different from the numerical simulations, the observational O_3 isopleths diagrams include all processes, such as transport, deposition and mixing, in addition to chemical reactions that control the ozone concentration. Accordingly, we selected the days when the sum of the hourly solar radiation data from sunrise to 18:00 exceeds the annual average, so as to reduce the influence of irregular solar intensity, and when the average wind speed data from sunrise to 18:00 is $<3ms^{-1}$, so as to reduce the influence of transport. For the NOx and VOCs concentrations to generate the O_3 isopleths diagrams, the average concentrations of VOCs and NOx in the daytime(6:00-9:00)are used, and the amount of ozone increase ($\triangle O_3$)is defined as the difference between the maximum value in (10:00-18:00) and the average value in the daytime (6:00-9:00)(Fig.7, left panel), the 8h O_3max is defined as the maximum ozone value during the time between 10:00-18:00(Fig.7, right panel). Fig.7 shows that when the VOCs concentration is between 0ppbc and 250ppbc, the ozone formation regime is VOC-limited, thus reducing the emissions of VOCs may reduce ozone formation; when the VOCs concentration is between 250ppbc and 600ppbc, the ozone formation regime is under NOx-limited and reduction of the emissions of NOx may reduce ozone formation; and when the VOCs concentration is above 600ppbc, the ozone formation regime is the (VOC and NOx)-limited regime, and reducing the VOCs and NOx together may reduce ozone formation. Ozone formation regime by VOCs concentrations may be decided by the composition of VOCs. Assuming that more active organic carbons are included in the VOCs composition, they are reacted with OH radicals more active than other hydrocarbons and the chain propagating reaction ($OH+RH \rightarrow R+H_2O$) would be more dominant than the chain terminating reaction (OH+NO2(+M)→HNO3(+M). We select the day (2011.8.12) represented by A point and the day (2011.11.5) represented by B point in Fig.7 (left panel. Alkanes, alkenes and aromatics are accounting for 50%, 18% and 32% of the total VOCs respectively on the day (2011.8.12), while alkanes, alkenes and aromatics are accounting for 58%, 17% and 25% of the total VOCs respectively on the day (2011.11.5), more active organic carbons are included in the VOCs composition on the day (2011.8.12). As a result, you can see lower VOCs concentration on the day (2011.8.12)can produce the same $\triangle O_3$ as the day(2011.11.5) with higher VOCs concentration, though other factors like meteorology should be taken into account for this. The high $\triangle O_3$ and 8h O_3max usually occur in the NOx-limited regime, which indicates that NO_x emissions must be controlled to regulate the occurrence of high-concentration ozone events. Fig.8 shows the scatters between VOCs and NOx selected by meteorological conditions in different seasons, most of the scatters under

NOx-limited and (VOC and NOx)-limited regimes correspond to summer and autumn, in which the high ozone episodes usually occur, strengthening the result that when the ozone concentration is very high, the ozone formation regime is NOx-limited. NOx emission control was of importance for peak ozone reduction in Guangzhou City.

In the formation of the tropospheric ozone, the reaction of VOCs and NO_x with free radicals plays an important role and the ozone formation relies on VOC/NO_x ratio. The numerical simulations showed that although the specific actual situations differ, it is generally considered that when the VOC/NOx ratio is greater than 8:1, the ozone formation regime is NOx-limited, and when the VOC/NOx ratio is less than 8:1, the ozone formation regime is VOC-limited (Dodge, 1977). This has been adopted and applied by many researchers during their researches throughout the world (Sillman, 1999; Committee on Tropospheric Ozone Formation and Measurement, 1991; Ran et al., 2009, 2011). In order to further prove the point we made earlier, the VOCs/NOx ratio (8) was used to judge the ozone formation regime, as it should provide a rough idea as to whether it is a NOx-sensitive or VOC-sensitive environment. Most previous studies in the PRD region reported that the ozone was VOC-limited(Zhang et al., 2008b; Guo et al., 2009). However, few previous studies regarding the region's ozone formation regime have examined the possible diurnal variations in ozone formation regime. An analysis was carried out on the diurnal variation of seasonal ozone concentration and the VOC/NO_x ratio during the monitoring period (Fig. 9). It was found that high-concentration ozone events are prone to occur in the summer and autumn. According to the traditional theory,in the morning (7:00 to 08:00 LT), the VOC/NO_x ratio is less than 8, the ozone formation regime is likely to be VOC-limited regime, and a decline in VOCs concentration would help to further reduce the ozone concentration. However, when the ozone concentration reaches a peak at noon, the VOC/NO_x ratio is greater than 8, and the ozone formation regime is likely to be NO_x-limited. The ozone formation regime can shift from VOC-limited in early the morning to NOx-limited at noon. The NO_x emissions must be controlled to achieve the purpose of controlling high-concentration ozone events, which is similar to the research findings in the Pearl River Delta (Li et al., 2013). In the spring and winter, the VOC/NO_x ratio is always less than 8, and ozone formation regime is likely to be VOC-limited for a long period of time. Since the ozone concentration is relatively low in these two seasons, although the control of NO_x emissions can increase the ozone concentration, no high-concentration ozone event will occur. Therefore, for the control of the local ozone, in addition to VOCs control, the control of NO_x concentration will further reduce high ozone concentration to prevent the occurrence of high-concentration ozone events, which to some extent may prove the point that we showed before. Considering the impact of VOCs to ozone formation is more relevant to the reactivity of individual VOC species rather than to the amount of VOCs, the VOC(reactivity)/NOx ratio was used to analyze ozone formation(Fig.9), the VOC(reactivity)/NOx ratio(PE or MIR) was shown to be consistent with the VOC(ppbc)/NOx ratio may due to the fact that regardless of the large variation in concentration of the three types of VOCs, the relative contribution of the three groups remains fairly uniform throughout the observational time(Fig.2). The high-concentration ozone is seriously harmful to human health, thus many regulators are focusing on reducing emissions at peak ozone forming hours (Castellanos et al., 2009). In order to further study the relationship of VOCs and NOx to the photochemical ozone production under the conditions

of high-concentration ozone, the days with high-concentration ozone were selected for analysis in the monitoring period; days with high-concentration ozone refers to the days with an hourly ozone value higher than 93 ppbv. It may be seen in Fig. 10 that under the conditions of high-concentration ozone at noon, the control of NO_x concentration may transiently reduce the peak of high-concentration ozone. However, when the ozone concentration is relatively low in the morning and at night, the control of the NO_x concentration may transiently increase the ozone concentration. Therefore, when high-concentration ozone events occur, more attention must be paid to controlling NO_x emissions, so as to achieve the purpose of controlling high-concentration ozone events.

4 Conclusions

One-year (from June 2011 to May 2012) consecutive observation was carried out on the near-surface ozone and its precursors VOCs and NO_x at GPACS, which is located in suburban Guangzhou where the high ozone events often occur. Observation-based analysis has been performed to investigate the relationship of VOCs and NOx on photochemical ozone production in this highly populated region.

The ozone concentration is significantly shown as being lower in the spring and winter and higher in the summer and autumn, while the precursors VOCs and NO_x display the opposite seasonal variation against the ozone. A negative growth of ozone concentration occurs between 15:00-18:00LT and 19:00-23:00LT. The first period of time (15:00-18:00LT) is presumably due to low OH radicals and the fact that titration of ozone by emissions of NOx plays a key role, while the second period of time is due to the fact that there was no OH radicals and NO titration could still consume the ozone .The photochemical reaction is intensive at noon, so that the variation trend of the ozone concentration shows a positive growth, and the photochemical formation of the ozone is larger than its chemical loss.

In terms of volume mixing ratio concentration and carbon number of VOCs, alkanes and aromatics are the most important atmospheric categories at the sampling site. As viewed from ozone formation potential, aromatics are the species with the largest contributions. Among these, toluene, m-xylene, p-xylene and 1,3,5-trimethylbenzene are the most important, with a total contribution to ozone formation potential of about 31.6 %. It should be noted that the concentration of isoprene emitted by plants is not high, but has a very large contribution to the ozone.

The ozone isopleths diagrams by measured data are employed to determine the ozone formation regime. When the VOCs concentration is between 0ppbc and 250ppbc, the ozone formation regime is VOC-limited; when the VOCs concentration is between 250ppbc and 600ppbc, the ozone formation regime is NOx-limited; and when the VOCs concentration is above 600ppbc, the ozone formation regime is (VOC and NOx)-limited regime. The high $\triangle O_3$ and 8h O_3max usually occur in NOx-limited which indicated that NO_x emissions must be controlled to regulate the occurrence of high-concentration ozone events in summer and autumn. This phenomenon is further confirmed by the measured VOCs/NOx, which shows that the ozone formation regime can shift from VOC-limited in early the morning to NOx-limited at noon in the summer and autumn, and the NO_x emissions must be controlled to achieve the purpose of controlling high-concentration ozone events; however, in the spring and winter, the ozone formation regime is VOC-limited for a long period of time. Since the ozone concentration is relatively low in these two seasons, although the control of the NO_x

emissions can increase the ozone concentration, no high-concentration ozone event will occur. It should be noted that the results are presented above only by observational data, and further investigations based on numerical model are needed in the future to obtain more detailed and robust conclusions. Numerical models currently available for simulating ozone pollution in the atmosphere, such as observation-based model (OBM), Weather Research and Forecasting-Chemistry mode (WRF-Chem) and U.S. Environmental Protection Agency's Community Multi-scale Air Quality (CMAQ), are necessary to analyze the formation of ozone from VOCs and NOx.

Acknowledgements This research work is funded by the National Natural Science Foundation of China (41175117, 40875090), National "973" Program (2011CB403400), Natural Science Foundation of Guangdong Province (S2012010008749), Special Research Project of Public Service Sectors (Weather) (GYHY201306042), and Science and Technology Sponsorship Program of Guangdong Province (2010A030200012)

References

Atkinson, R. and Arey, J.: Atmospheric degradation of volatile organic compounds, Chem. Rev., 103, 4605–4638, 2003.

Bloomer, B. J., Stehr, J. W., Piety, C. A., Ross, J. S., and Dickerson, R. R.: Observed relationships of ozone air pollution with temperature and emissions, Geophys. Res. Lett., 36, L09803, doi:10.1029/2009GL037308, 2009.

Bloomer, B. J., Vinnikov, K. Y., and Dickerson, R. R.: Changes in seasonal and diurnal cycles of ozone and temperature in the eastern US, Atmos. Environ., 44, 1–9, 2010.

Carter, W. P. L.: Development of ozone reactivity scales for volatile organic compounds, J. Air Waste Manage., 44, 881–899, 1994.

Castellanos, P., Stehr, J. W., Dickerson R. R., and Ehrman, S. H.: The sensitivity of modeled ozone to the temporal distribution of point, area, and mobile source emissions in the eastern United States, Atmos. Environ., 43, 4603–4611, 2009.

Chan, C. K. and Yao, X. H.: Air pollution in mega cities in China, Atmos. Environ., 42, 1–42, doi:10.1016/j.atmosenv.2007.09.003, 2008.

Cheng, H. R., Guo, H., Saunders, S. M., Lam, S. H. M., Jiang, F., Wang, X. M., Simpson, I. J., Blake, D. R., Louie, P. K. K., andWang T. J.: Assessing photochemical ozone formation in the Pearl River Delta with a photochemical trajectory model, Atmos. Environ., 44, 4199–4208, 2010.

Committee on Tropospheric Ozone Formation and Measurement: Rethinking the Ozone Problem in Urban and Regional Air Pollution, Natl. Acad. Press, Washington, DC, 1991.

Deng, X. J., Wang, X. M., Zhao, C. S., Ran, L., Li, F., Tan, H. B., Deng, T., Wu, D., and Zhou, X. J.: The mean concentration and chemical reactivity of VOCs of typical processes over Pearl River Delta Region, China, Environ. Sci., 30, 1153–1161, 2010.

Dodge, M. C.: Combined use of modeling techniques and smog chamber data to derive ozone precursor relationships, Proceedings of the international conference on photochemical oxidant pollution and its control, 2, 881–889, 1977.

Geng, F. H., Tie, X. X., Xu, J. M., Zhou, G. Q., Peng, L., Gao, W., Tang, X., and Zhao, C. S.: Characterizations of ozone, NO_x, and VOCs measured in Shanghai, China, Atmos. Environ., 42, 6873–6883, 2008.

Guo, H., Jiang, F., Cheng, H. R., Simpson, I. J., Wang, X. M., Ding, A. J., Wang, T. J., Saunders, S. M., Wang, T., Lam, S. H. M., Blake, D. R., Zhang, Y. L., and Xie, M.: Concurrent observations of air pollutants at two sites in the Pearl River Delta and the implication of regional transport, Atmos. Chem. Phys., 9, 7343–7360, doi:10.5194/acp-9-7343-2009, 2009.

Li, Y.: Numerical Studies on Ozone Source Apportionment and Formation Regime and their Implications on Control Strategies, Hong Kong University of Sci. & Tech., Hong Kong, 2011.

Li, Y., Lau, K. H., Fung, C. H., 5 Zheng, J. Y., and Liu, S. C.: Importance of NO_x control for peak ozone reduction in the Pearl River Delta region, J. Geophys. Res., 118, 9428–9443, 2013.

Liu, Y., Shao, M., Fu, L. L., Lu, S. H., Zeng, L. M., and Tang, D. G.: Source profiles of volatile organic compounds (VOCs) measured in China: part I, Atmos. Environ., 42, 6247–6260, 2008.

Ran, L., Zhao, C. S., Geng, F. H., Tie, X. X., Xu, T., Li, P., Guang, Q. Z., Qiong, Y., Xu, J. M., and Guenther, A.: Ozone photochemical production in urban Shanghai, China: analysis based on ground level observations, J. Geophys. Res., 114, doi:10.1029/2008JD010752, 2009.

Ran,L.,Zhao,C.S.,Xu,W.Y.,Lu,X.Q.,Han,M.,Lin,W.L.,Yan,P.,Xu,X.B.,Deng,Z.Z.,Ma,N.,Liu,P.F.,Yu,J. ,Liang,W.D., and Chen, L.L.:VOC reactivity and its effect on ozone production during the HaChi

summer campaign, Atmos. Chem. Phys., 11,4657–4667, doi:10.5194/acp-11-4657-2011, 2011.

Shao, M., Zhang, Y. H., Zeng, L. M., Tang, X. Y., Zhang, J., Zhong, L. J., and Wang, B. G.: Ground-level ozone in the Pearl River Delta and the roles of VOC and NO_x in its production, Environ. Manage., 90, 512–518, 2009. Sillman, S.: The use of NO_y, H_2O_2, and HNO_3 as indicators for ozone-NO_x-hydrocarbon sensitivity in urban locations, J. Geophys. Res., 100, 14175–14188, 1995.

Sillman, S.: The relation between ozone, NO_x and hydrocarbons in urban and polluted rural environment, Atmos. Environ., 33, 1821–1845, 1999.

Tie, X., Madronich, S., Li, G. H., Ying, Z. M., Zhang, R. Y., Garcia, A. R., Taylor, J. L., and Liu, Y. B.: Characterizations of chemical oxidants in Mexico City: a regional chemical/ dynamical model (WRF-Chem) study, Atmos. Environ., 41, 1989–2008, 2007.

Wang, B. G., Zhang, Y. H., and Shao, M.: Special and temporal distribution character of VOCs in the ambient air of Pearl River Delta region, Environ. Sci., 25, 7–15, 2004.

Wang, T., Wei, X. L., Ding, A. J., Poon, C. N., Lam, K. S., Li, Y. S., Chan, L. Y., and Anson, M.: Increasing surface ozone concentrations in the background atmosphere of Southern China, 1994–2007, Atmos. Chem. Phys., 9, 6217–6227, doi:10.5194/acp-9-6217-2009, 2009.

Wang, T. J., Jiang, F., Deng, J. J., Shen, Y., Fu, Q. Y., Wang, Q., Fu, Y., Xu, J. H., and Zhang, D. N.: Urban air quality and regional haze weather forecast for Yangtze River Delta region, Atmos. Environ., 58, 70–83, 2012.

Wang, X. M., Carmichael, G., Chen, D. L., Tang, Y. H., and Wang, T. J.: Impacts of different emission sources on air quality during March 2001 in the Pearl River Delta (PRD) region, Atmos. Environ., 39, 5227–5241, 2005.

Zhang, R. Y., Lei, W. F., Tie, X. X., and Hess, P.: Industrial emissions cause extreme diurnal urban ozone variability, P. Natl. Acad. Sci. USA, 101, 6346–6350, 2004.

Zhang, Y. H., Su, H., Zhong, L. J., Cheng, Y. F., Zeng, L. M., Wang, X. S., Xiang, Y. R., Wang, J. L., Gao, D. F., and Shao, M.: Regional ozone pollution and observation-based ap-proach for analyzing ozone–precursor relationship during the PRIDE-PRD2004 campaign, Atmos. Environ., 42, 6203–6218, doi:10.1016/j.atmosenv.2008.05.002, 2008.

Zhao, P. S., Zhang, X. L., Xu, X. F., and Zhao X. J.: Long-term visibility trends and characteristics in the region of Bejing, Tianjin, and Hebei, China, Atmos. Res., 101, 711–718, 2011.

Zou, Y., Deng, X. J., Wang, B. G., Li, F., and Huang, Q.: Pollution characteristics of volatile organic compounds in Panyu Composition Station, Environ. Sci., 33, 808–813, 201

Table 1. The wind speed and temperature in four seasons (from June 2011 to May 2012) at GPACS.

		Minimum	Maximum	Mean value	Median
Spring	Windspeed/ms^{-1}	0	5.4	1.3	1.2
	Temperature/℃	9.4	35.5	22.6	22.9
Summer	Windspeed/ms^{-1}	0	6.0	1.4	1.2
	Temperature/℃	23.9	37.1	29.4	28.8
Autumn	Windspeed/ms^{-1}	0	5.7	1.5	1.4
	Temperature/℃	16.2	35.3	25.2	25.2
Winter	Windspeed/ms^{-1}	0	6.3	1.5	1.4
	Temperature/℃	4.7	26.9	14.2	14.1

Table 2. The standard curve and detection line of VOC species

Target compound	Standard curve	correlation coefficient	Detection limit (ppbv)
Ethylene	y=1.0188x+0.2659	0.997	0.07
Acetylene	y=1.0409x+0.1756	0.998	0.08
Ethane	y=1.0162x+0.2891	0.997	0.08
Propylene	y=0.9959x+0.1506	0.999	0.07
Propane	y=0.9824x+0.2082	0.998	0.09
Isobutane	y=0.9753x+0.3785	0.994	0.05
1-Butene	y=0.9587x+0.3641	0.994	0.06
n-Butane	y=0.9776x+0.3718	0.994	0.05
t-2-Butene	y=0.9746x+0.2747	0.997	0.05
c-2-Butene	y = 0.9834x+0.1606	0.999	0.06
Isopentane	y=0.9753x+0.2135	0.998	0.07
1-Pentene	y = 0.919x+0.1626	0.998	0.05
n-Pentane	y = 0.9557x+0.2038	0.984	0.07
Isoprene	y=1.0304x+0.1653	0.998	0.07
trans-2-pentene	y=0.9753x+0.2135	0.998	0.07
cis-2-pentene	y = 0.9557x+0.2038	0.984	0.07
2,2-Dimethylbutane	y=0.9731x+0.1971	0.998	0.07
Cyclopentane	y=0.9993x+0.1412	0.997	0.06
2,3-Dimethylbutane	y = 0.919x+0.1626	0.999	0.07
2-Methylpentane	y = 0.9557x+0.2038	0.984	0.07
3-Methylpentane	y=0.9753x+0.2135	0.998	0.07
2-Methyl-1-Pentene	y=0.9700x+0.3300	0.995	0.05
n-Hexane	y=0.9915x+0.2626	0.997	0.06
Methylcyclopentane	y = 0.9749x+0.1832	0.999	0.07
2,4-Dimethylpentane	y=0.9993x+0.1412	0.999	0.05
Benzene	y=0.9753x+0.2835	0.997	0.06
Cyclohexane	y=0.9841x+0.2744	0.997	0.07
2-methylhexane	y=0.9744x+0.2979	0.996	0.05
2,3-dimethylpentane	y=0.9779x+0.2953	0.997	0.05
3-methylhexane	y=0.9735x+0.3374	0.995	0.05
2,2,4-trimethylpentane	y=0.9696x+0.3947	0.994	0.05
n-Heptane	y=0.9678x+0.3635	0.994	0.05
Methylcyclohexane	y=0.9819x+0.3629	0.995	0.05
2,3,4-trimethylpentane	y=0.9691x+0.3994	0.994	0.04
Toluene	y=0.9696x+0.3397	0.995	0.05
2-methylheptane	y=0.9603x+0.4835	0.990	0.04
3-methylheptane	y=0.9625x+0.4550	0.991	0.04
n-Octane	y=0.9524x+0.5082	0.989	0.04
Ethylbenzene	y=0.9629x+0.4253	0.992	0.04

m&p-Xylenes	y=0.9541x+0.5844	0.986	0.03
Styrene	y=0.9524x+0.4132	0.991	0.04
o-Xylene	y=0.9515x+0.4926	0.989	0.04
n-Nonane	y = 0.9878x+0.1635	0.998	0.04
Isopropylbenzene	y=0.9418x+0.5162	0.986	0.04
n-Propylbenzene	y=0.9426x+0.5468	0.986	0.04
m-Ethyltoluene	y = 0.9532x+0.4838	0.989	0.04
p-Ethyltoluene	y = 0.9554x+0.3953	0.992	0.04
1,3,5-Trimethylbenzene	y = 0.951x+0.4724	0.989	0.04
o-Ethyltoluene	y = 0.9784x+0.0956	0.999	0.04
1,2,4-trimethylbenzene	y = 0.9563x+0.4509	0.991	0.03
n-Decane	y = 0.9651x+0.3068	0.995	0.04
1,2,3-trimethylbenzene	y = 0.9537x+0.3191	0.993	0.04
m-Diethylbenzene	y = 0.9541x+0.4494	0.991	0.04
p-Diethylbenzene	y = 0.9607x+0.3788	0.993	0.04
n-Undecane	y = 0.9519x+0.3329	0.992	0.04

Table 3. Daily average of VOCs and its constituents, NOx and ozone in four seasons（from June 2011 to May 2012）at GPACS

		Alkanes/ ppbv	Alkenes/ ppbv	Aromatics /ppbv	VOCs/ ppbv	NOx/ ppbv	O_3/ ppbv
	March	20.84	5.26	8.50	34.60	76.39	12.46
Spring	April	25.11	5.86	11.33	42.30	35.17	16.02
	May	21.45	5.47	10.94	37.86	25.29	24.55
	June	19.74	6.62	14.23	40.60	24.40	24.26
Summer	July	20.07	6.72	12.90	39.69	24.70	24.26
	August	22.36	9.12	9.99	41.46	21.75	28.26
	September	20.82	7.80	8.95	37.57	25.18	29.67
Autumn	October	22.26	5.63	8.89	36.78	26.59	25.34
	November	39.16	10.24	14.16	63.57	39.98	21.78
	December	33.61	8.47	5.97	48.05	39.14	20.37
Winter	January	32.13	7.96	7.54	47.63	34.82	9.31
	February	-	-	-	-	52.69	9.97

Table 4. Photochemical properties of VOCs and their average mixing ratios at GPACS from June 2011 to May 2012.

Compound	MIR[a]	$K^{b}_{OH} \times 10^{12}$	Mixing ratio （ppbv）	Mixing ratio （ppbc）
Alkanes				
Ethane	0.25	0.27	3.66	7.31
Propane	0.46	1.15	4.34	13.02
i-Butane	1.18	2.34	2.67	10.68
n-Butane	1.08	2.54	3.07	12.28
Cyclopentane	2.24	5.16	0.15	0.77
i-Pentane	1.36	3.9	1.72	8.61
n-Pentane	1.22	3.94	1.37	6.86
Methylcyclopentane	1.46	5.1	0.32	1.94
2,3-Dimethylbutane	1.07	6.3	0.13	0.76
2-Methylpentane	1.4	5.6	0.88	5.29
3-Methylpentane	1.69	5.7	0.75	4.51
n-Hexane	1.14	5.6	1.43	8.56
2,4-Dimethylpentane	1.11	5.7	0.37	0.41
Cyclohexane	1.14	7.49	1.65	9.90
2-Methylhexane	1.09	6.9	0.58	4.04
2,3-Dimethylpentane	1.25	5.1	0.26	1.82
3-Methylhexane	1.5	5.1	0.52	3.66
2,2,4-Trimethylpentane	1.2	3.68	0.22	1.79
n-Heptane	0.97	7.15	0.32	2.24
Methylcyclohexane	1.56	10.4	0.26	1.81
2,3,4-Trimethylpentane	0.97	7	0.12	0.96
2-Methylheptane	1.12	8.3	0.08	0.66
3-Methylheptane	0.8	8.6	0.08	0.68
n-Octane	0.68	8.68	0.19	1.54
n-Nonane	0.59	10.2	0.35	3.18
n-Decane	0.52	11.6	0.03	0.29
n-Undecane	0.47	13.2	0.17	1.92
n-Dodecane	0.38	14.2	0.14	1.65
Alkenes				
Ethene	7.4	8.5	2.99	5.97
Propene	11.57	26.3	1.32	3.96
trans-2-Butene	15.2	64	0.28	1.14
1-Butene	9.57	31.4	0.44	1.77
cis-2-Butene	14.26	56.4	0.22	0.86
trans-2-Pentene	10.47	67	0.03	0.15
1-Pentene	7.07	31.4	0.05	0.23
cis-2-Pentene	10.28	65	0.19	0.97
Isoprene	10.48	101	1.14	5.72

1-Hexene	—	—	0.67	3.99
Aromatics				
Toluene	3.93	5.96	4.59	32.10
Ethylbenzene	2.96	6.96	1.48	11.81
m,p-Xylene	8.54	20.5	1.41	11.24
Styrene	1.66	58	0.41	3.25
o-Xylene	7.58	13.6	0.66	5.28
i-Propylbenzene	2.45	6.6	0.10	0.86
n-Propylbenzene	1.96	5.7	0.23	2.05
m-Ethyltoluene	7.39	18.6	0.25	2.22
p-Ethyltoluene	4.39	11.8	0.21	1.89
1,3,5-Trimethylbenzene	11.75	56.7	0.21	1.86
o-Ethyltoluene	5.54	11.9	0.27	2.47
1,2,4-Trimethylbenzene	8.83	32.5	0.21	1.92
1,2,3-Trimethylbenzene	11.94	32.7	0.15	1.32
m-Diethylbenzene	7.08	15	0.12	1.25
p-Diethylbenzen	4.39	10	0.11	1.05

MIR[a] denotes maximum incremental reactivity（Carter, et al., 1994)

k^{b}_{OH} denotes rate constant of VOCs react with hydroxyl radicals at 298K,(Atkinson and Arey,2003)

Table 5. Top 10 VOCs species at GPACS based on the Propy-Equiv and MIR scales from June 2011 to May 2012.

OH Reactivity Rank		MIR Rank	
Compound	Percentage（%）	Compound	Percentage（%）
Isoprene	19.97	Toluene	16.26
m,p-Xylene	7.97	m,p-Xylene	12.48
Toluene	6.62	Isoprene	7.99
Styrene	6.51	Propene	6.30
1,3,5-Trimethylbenzene	3.82	Ethene	6.07
Propene	3.60	o-Xylene	5.21
Ethylbenzene	2.85	Ethylbenzene	4.54
Cyclohexane	2.56	1,3,5-Trimethylbenzene	2.87
trans-2-Butene	2.51	trans-2-Butene	2.37
o-Xylene	2.48	1,2,4-Trimethylbenzene	2.22

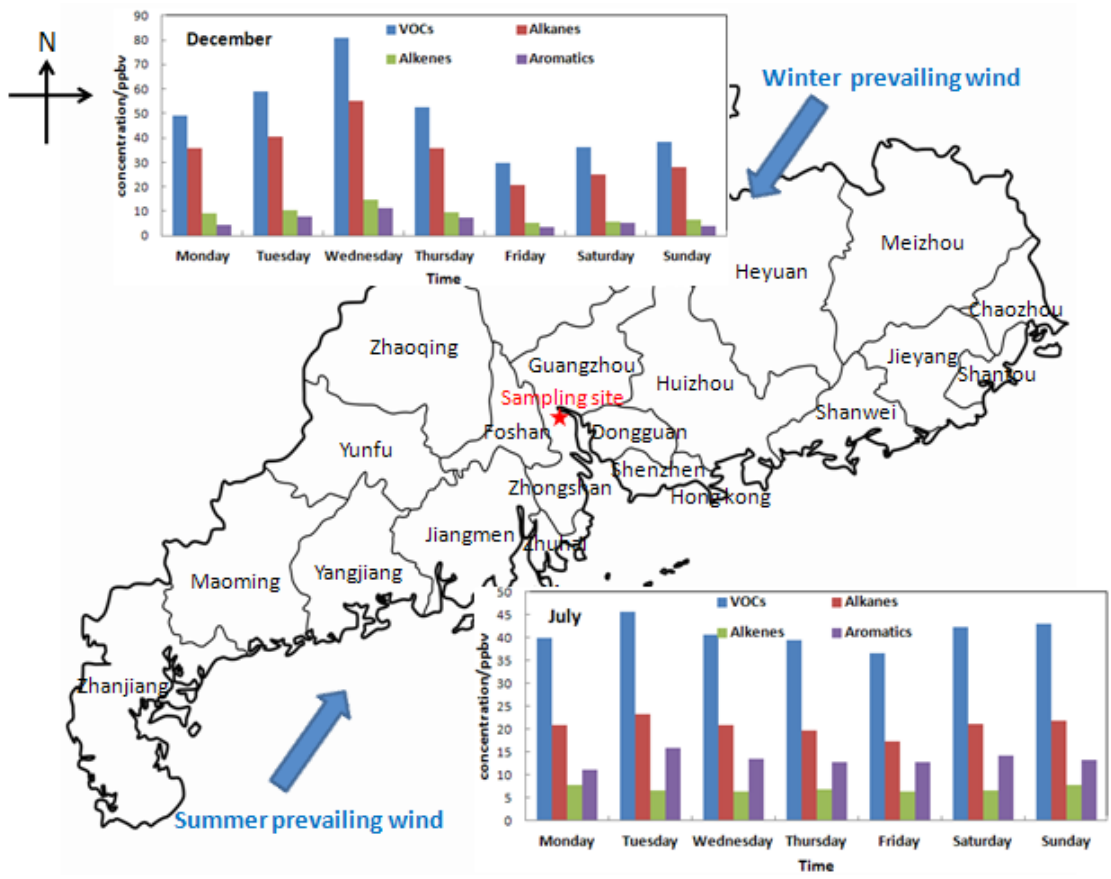

Figure 1. The location of observation site at GPACS and its surrounding area, the pentagram represents the sampling site. The VOCs concentration in July when the summer prevailing wind is southwesterly and in December when the winter prevailing wind is northeasterly is showed in the map.

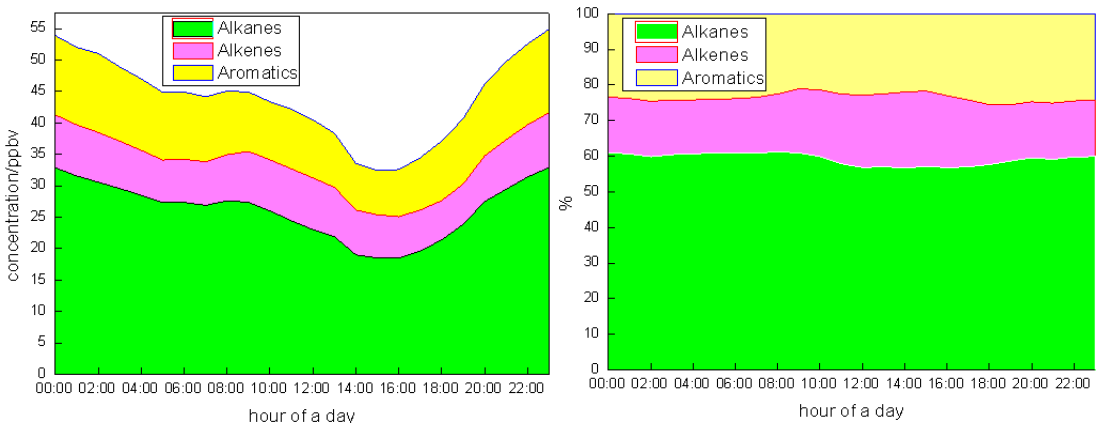

Figure 2. Daily cycle of hourly averaged concentration of three categories of VOCs in ppbv and in % of total (from June 2011 to May 2012) at GPACS

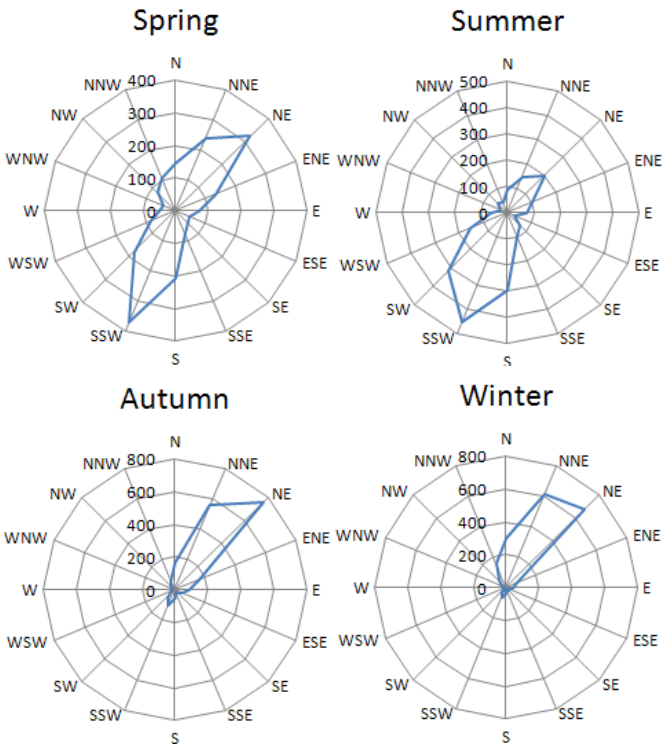

Fig 3. The frequency of wind direction plotted by wind rose for four seasons（from June 2011 to May 2012）at GPACS

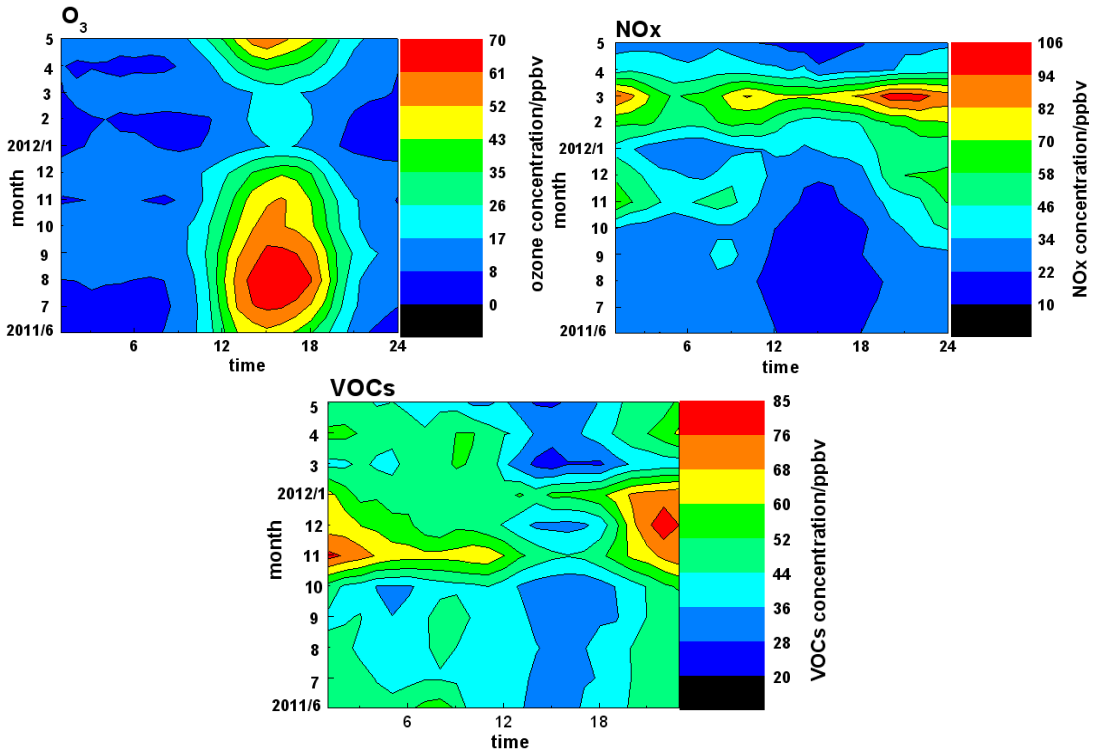

Fig 4. The diurnal variations of ozone, NOx and VOCs in months（from June 2011 to May 2012）at GPACS.

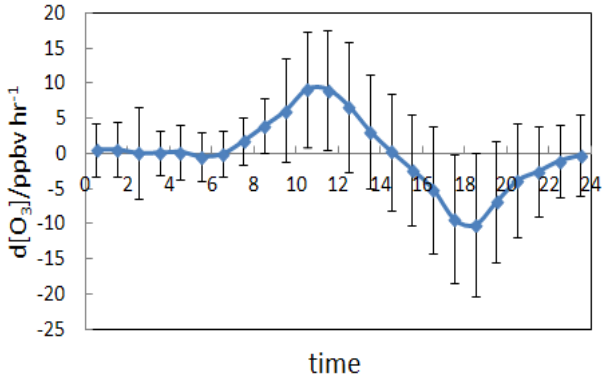

Fig 5. Average diurnal trends in ozone from June 2011 to May 2012 at GPACS. Colored marker represents hourly mean value. The black line gives the standard deviation.

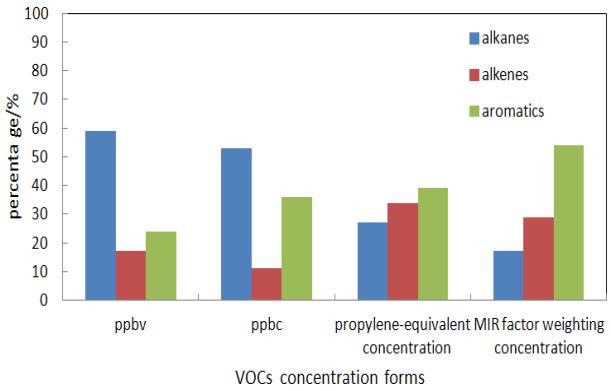

Fig 6. Average fractions of each category based on volume mixing ratio (ppbv), carbon-atom-based concentration (ppbc), OH-reactivity-based Propy-Equiv concentration (ppbc), and MIR factor weighting concentration(ppbv). Fractions of each VOCs category（alkanes, alkenes and aromatics）plotted by bar based on four methods (ppbv, ppbc, propylene-equivalent concentration and MIR factor weighting concentration) from June 2011 to May 2012 at GPACS.

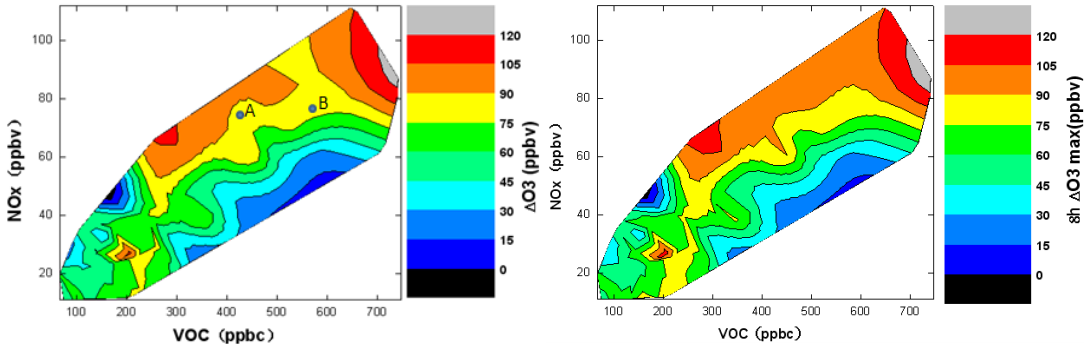

Fig 7. O_3 isopleth diagrams plotted by observational data from June 2011 to May 2012 about the amount of O_3 increase($\triangle O_3$)（left panel）and 8h O_3max（right panel）. The observational data are selected by the days when the sum of the solar radiation from sunrise to 18:00 exceeds the annual average and when the average wind speed from sunrise to 18:00 $<$ 3ms^{-1}. The average concentrations of VOCs and NOx in the daytime (6:00-9:00) are used, and the amount of O_3 increase($\triangle O_3$)is defined as the difference between the maximum value in (10:00-18:00) and the average value in the early morning (6:00-9:00), the 8h O_3max is defined as the maximum during the time between 10:00-18:00. A point represents the day (2011.8.12) and B point represents the day (2011.11.5).

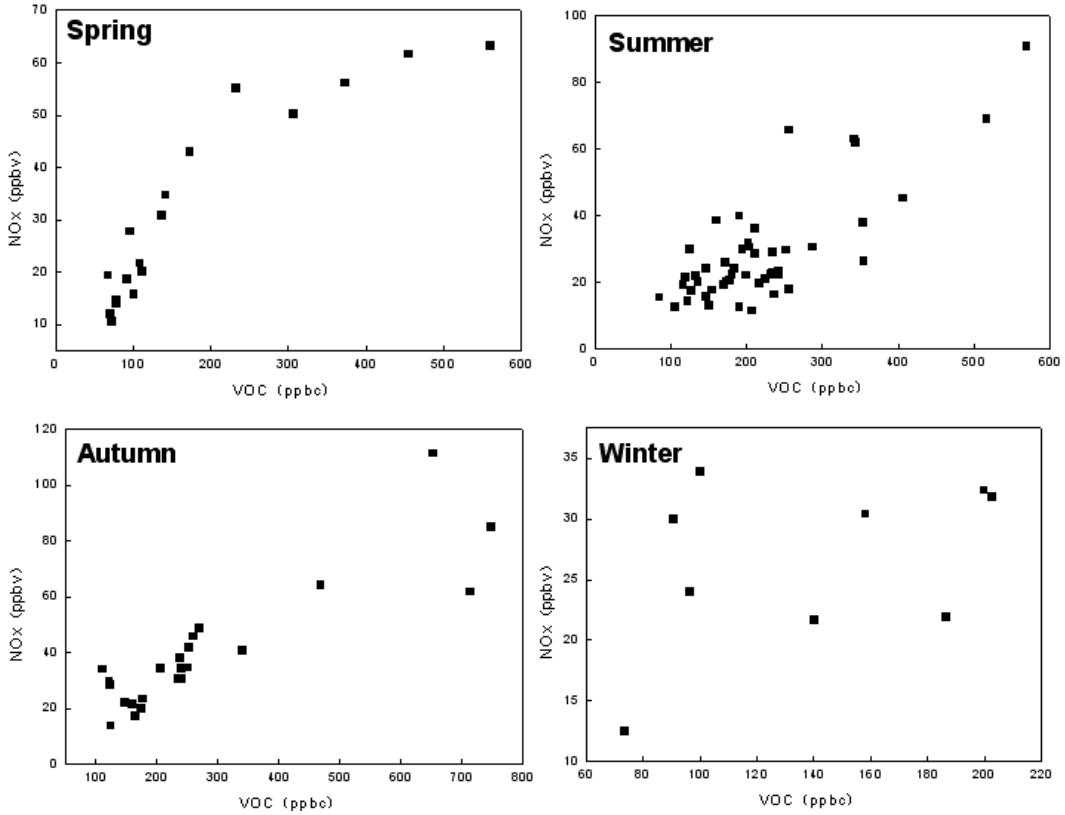

Fig 8. The scatter diagram between VOCs and NOx by observational data from June 2011 to May 2012 selected by the days when the sum of the solar radiation from sunrise to 18:00 exceeds the annual average and when the average wind speed from sunrise to 18:00＜3ms^{-1}.

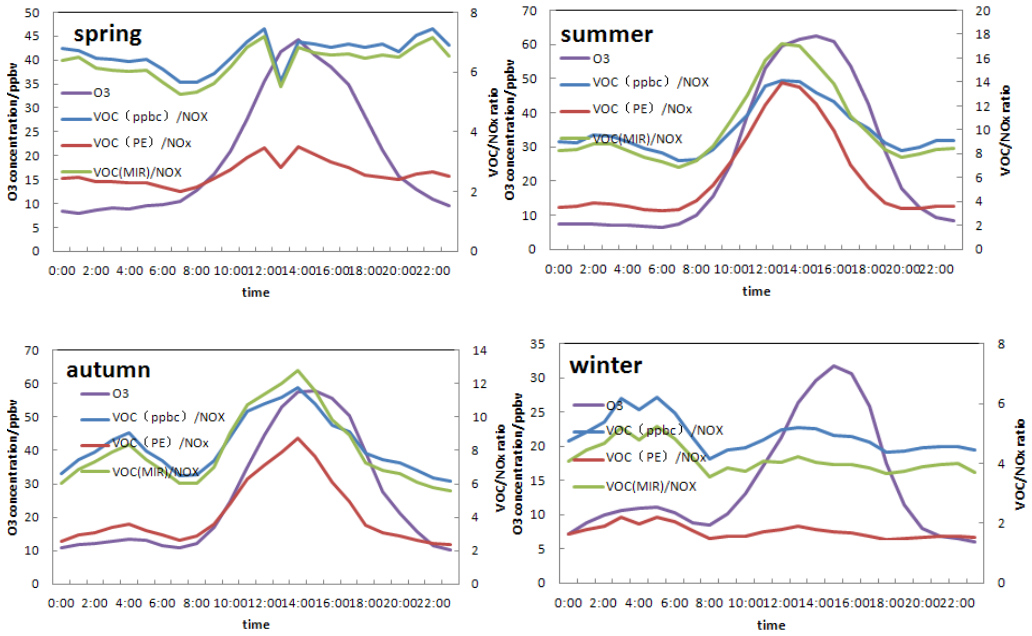

Figure 9. The variation patterns of VOC/NOx ratio and ozone concentration at four seasons（from June2011 to May 2012）at GPACS. Three forms of VOC（ppbc, PE and MIR）is presented by blue, red and green respectively and colored markers represent hourly mean value.

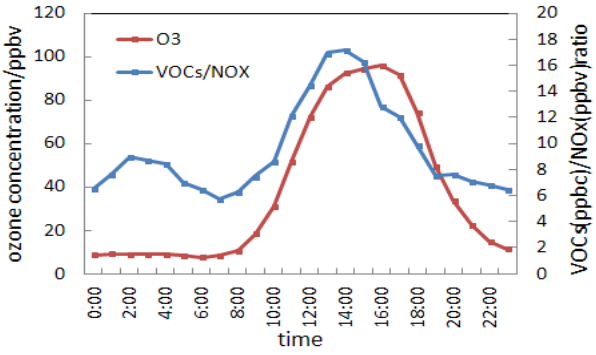

Fig 10. The variation patterns of VOC/NOx ratio and ozone concentration at high ozone episode at GPACS. Colored markers represent hourly mean value. High ozone episode refers to the days with an hourly ozone value higher than 93ppbv.